Estimating heat stress in the urban centre of Košice using ENVI-met and high-resolution surface data

Tomáš FEDOR, Jaroslav HOFIERKA

Abstract: *This study employs the ENVI-met microscale model to assess heat stress in the urban core of Košice, Slovakia, during a heat wave on 30 June 2022. Utilising high-resolution surface data derived from Sentinel-2 multispectral imagery, LiDAR point clouds, and shapefiles, we quantify the Universal Thermal Climate Index (UTCI) to evaluate diurnal heat stress dynamics. The model incorporates detailed urban morphology, including buildings, 3D vegetation, and land cover, with meteorological forcing data from hourly SYNOP observations at the Košice airport. Results highlight significant heat stress in densely built-up areas, with UTCI peaks in the late afternoon due to high heat accumulation and low wind speeds. The study underscores the effectiveness of ENVI-met for high-resolution urban microclimate simulations and identifies hotspots for potential heat stress mitigation strategies.*

Keywords: *urban heat island, heat stress, ENVI-met, UTCI, Košice*

Introduction

Urban areas with large concentrations of human populations represent one of the most studied forms of anthropogenic microclimate modification. The most prominent impact of the urban areas lays in significant temperature increase caused by diurnal radiative overheating and heat retention of the built-up surfaces and materials, often with several Celsius degrees difference in air temperature between the urban and surrounding rural areas (Oke 1982). This phenomenon is also known as Urban Heat Island (UHI). Since the UHI is caused by surface overheating, it can be divided into Surface Urban Heat Island (SUHI) and Atmospheric Urban Heat Island (AUHI) formed consequently from heat transfer of the surface. AUHI can be further divided into Canopy Layer Urban Heat Island (CLUHI) and Boundary Layer Urban Heat Island (BLUHI) as categorized by Branea et al. (2016).

The SUHI and AUHI have different diurnal characteristics, with SUHI reaching the peak with highest radiative heating, while the AUHI have delayed maximum intensity during the afternoon and evening hours and tends to be more prone to prevailing atmospheric conditions (Fedor and Hofierka 2022). Estimating SUHI helps to determine thermal properties of the materials covering the urban surfaces and objects within the canopy layer and identify the hotspots with highest diurnal heating and heat retention during the night, which consequently influences the AUHI formation and characteristics.

There are various methods developed for detailed estimation of the SUHI including our recent research using the direct measurements of the surface temperature, remote sensing and physically based surface and radiation models (Hofierka et al. 2020a, Hofierka et al. 2020b, Onačillová et al. 2022). These methods can provide high-resolution surface temperature data, although they are limited when estimating the heat impact on populations in situations where other physiological (Foster et al. 2020, Meade et al. 2020) or environmental and atmospheric variables (Sobolewski et al. 2020, Xiao et al. 2020, Luo and Lau 2021) may influence overall heat stress.

https://doi.org/10.33542/GC2025-2-01

Atmospheric numerical weather prediction (NWP) and environmental computational fluid dynamics (CFD) models capable of simulating atmospheric processes within the CLUHI and BLUHI represent a very suitable method to cover the gap in estimating the heat stress (Cheval et al. 2021). Paired with high resolution urban surface data as input and sufficient computational resources, these models can simulate the dynamics of the urban microclimate in high resolution with multiple atmospheric and environmental variable outputs like ambient and radiant temperature, humidity, and wind speed, which are necessary for overall heat stress assessment (Oleson et al. 2013).

Various indicators are available for estimating heat stress, including simpler physically based indices such as the heat index, humidex, wet bulb globe temperature, and apparent temperature (Aghamohammadi and Santamouris 2022), as well as more complex indices like the Universal Thermal Climate Index (UTCI), Predicted Mean Vote (PMV), Physiological Equivalent Temperature (PET), and Standard Effective Temperature (SET), which also incorporate individual physiological parameters (Mahdavinejad et al. 2024).

ENVI-met represents one of the most widely used CFD models capable of simulating the urban climate in high resolution. Several studies in central European setting have demonstrated the model performance regarding thermal stress assessment and its potential as a viable tool in changing climate (Huttner et al. 2008). In the case study of the heat wave event in Lublin city in Poland by Kozak et al. (2023), the model correctly identified the maximum values of thermal stress using the UTCI. Facade orientation also plays an important role when estimating the radiation fluxes in dense built-up areas, strongly influencing the overall thermal stress, as in the study conducted by Kántor et al. (2018) in the Hungarian city of Szeged. Good performance of the model when estimating the thermal stress was also recorded in a study conducted by Maras et al. (2014) over the German city of Aachen, though with a stated limitation in model integration of the large-scale atmospheric processes.

The aim of this study is to apply the ENVI-met microscale model to assess heat stress in the urban core of Košice, using newly derived high-resolution surface input data. The focus is on quantifying the diurnal cycle of the UTCI heat stress index during the heat wave event on 30 June 2022, as well as evaluating the overall model performance based on key atmospheric variables derived from surface meteorological measurements.

Study area and heat wave selection

Košice is a city located in the eastern part of Slovakia, an inland country situated in central Europe (fig. 1). The city lies close to the border with Hungary and is part of the Košice Basin, a lowland region surrounded by upland and mountainous terrain. The city is positioned at approximately 48.72°N latitude and 21.25°E longitude, placing it within the warm, moderately dry climate region with mild winters according to the climatological classification by Lapin et al. (2002). The average annual temperature measured in the city of Košice reaches 8.6 °C (1961-1990) and average yearly precipitation values range in between 600-700 mm (1961-1990) (Lapin et al. 2002). Significant warming of climate in recent years also led to increased frequency of heat waves and their intensity in the study area (Lapin et al. 2016).

The city is located on the southern side of the Carpathian Mountains, between the Slanské vrchy (Slanské hills) to the east and the Volovské vrchy (Volovské hills) to the west, which significantly influences the regional climate and dynamics of the weather. These landfoms contribute to the city topographic enclosure from the sides and affect local wind patterns. The elevation of the city ranges between 200 to 250 meters above sea level with only slight elevation difference in the urban core located close to the Hornád river. The Hornád river flows through the central part of the city, including the part of the study area. It is mostly an open flat area characterised by residential buildings, industrial complexes and railway station. Surrounding vegetation includes urban greenery, agricultural land, and patches of forested hills,

all of which influence surface roughness, albedo, and evapotranspiration processes relevant for ENVI-met simulations.

Given its location and topographical context, Košice represents a complex urban microclimate system where orographic effects, land use patterns, and regional atmospheric influences converge. This makes it a suitable case study for high-resolution ENVI-met modelling focused on assessing urban heat island effects, thermal comfort or microclimatic interventions in a central European setting.

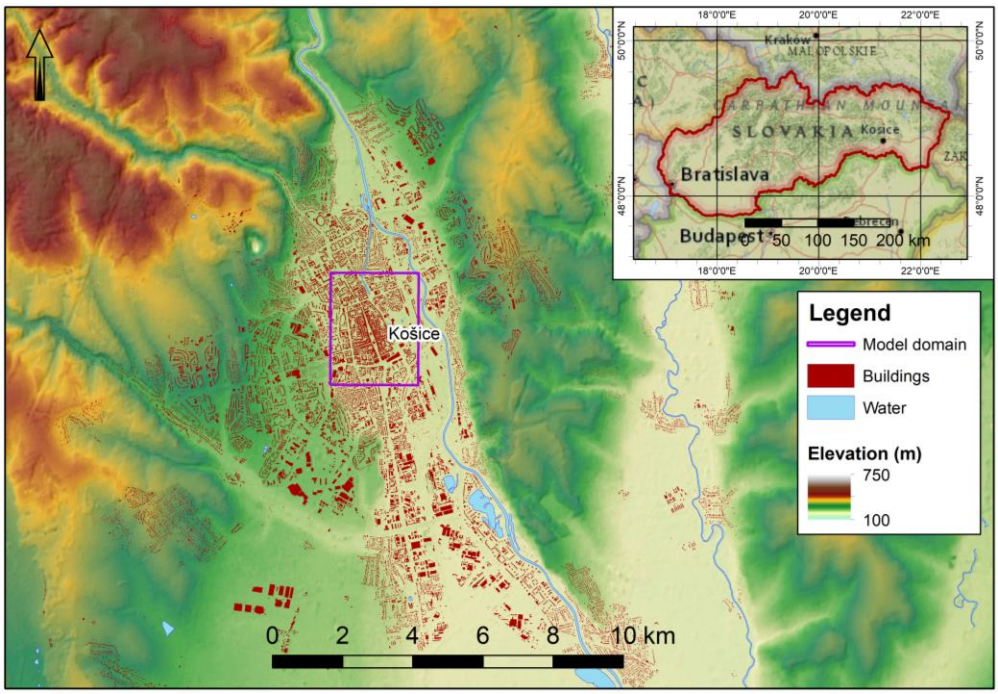

Fig. 1. *Localisation of the Košice city and the model domain representing the study area*

Analysing heat stress in urban areas under real weather scenarios requires the selection of an appropriate case study, since heat stress is influenced by multiple variables. Selecting the potentially highest heat stress scenario can be beneficial to test the model fully and potentially provide valuable data for mitigation strategies or future studies.

In this study we selected a typical heat wave event in central Europe with high temperature, low wind speed, moderate humidity and almost clear-sky conditions. Such situations are typical for backside of the upper-level ridge, with strong warm advection and relatively dry upper profile of the troposphere. This situation was also analysed from a meteorological point of view in our study over Košice city (Fedor and Hofierka 2022) using the numerical weather prediction model.

Meteorological inputs, or forcing data, play an important role when running the real case weather scenarios. The forcing data define the initial and boundary atmospheric conditions for the simulation. In ENVI-met, the forcing data for real case scenario are by default defined as inputs of temperature, relative humidity, precipitation, wind speed and direction and cloud cover or short-wave radiation obtained from surface measurements and observations in regular interval covering the simulation period.

The forcing data are usually obtained from weather stations. For our analysis, we selected a data from surface synoptic observations (SYNOP) measured hourly at the local airport

located to the south of the city (fig. 4). The maximum temperature reached at the airport was 36.0 °C during the afternoon hours of 30 June, and the minimum temperature was 21.1 °C in the morning of 1 July. The location of the stations allows for ingestion forcing data representing the rural area entering the urbanized model domain without the data contamination of the UHI plume advecting in the opposite direction. The data were selected for 29 June 2022 12:00 CET to 1 July 2022 0:00 CET to allow the proper model spin-up with diurnal heating and heat accumulation from the previous day and to cover the radiation cooling and maximum heat retention during the night between 30 June and 1 July.

Model and computational domain adjustments

ENVI-met represents a 3D, non-hydrostatic CFD model designed for atmospheric and environmental simulations. The model is focused on small-scale microclimatic simulations mostly within the boundary layer and is primarily designed for urban areas with applications in urban planning, air quality, and heat stress management. The model is characterized by high spatial resolution with a grid size between 0.5 and 99 meters and detailed plant, surface, and building processes occurring within the canopy layer.

This study aims to perform a high-resolution simulation for the urban centre of Košice. The model domain was configured with a horizontal grid resolution of 5 meters (343 × 434 grid cells) and a vertical resolution of 1 meter with 60 vertical levels. The model domain was defined to cover only the city core, avoiding the taller orography located on the edges of the city (fig. 1 and fig. 2). The taller orography would increase the model domain height and consequently demand more computational power required to run the simulation. To improve the stability of the model, a 5-grid nesting was also applied to the domain.

The forcing data were incorporated in hourly resolution with cloud amount used as forcing of the radiation. The model was set with default required parameterisation and time-step setting. The Bruse/ENVI-met 2017 was set as a turbulence model with enabled limitation of turbulent kinetic energy (TKE) for better model stability. Wind resistance at facades was parameterised with DIN 6946 method to include higher zero-level values. For better representation of the vegetation the tree calendar was enabled, incorporating the average phase of the tree foliage for the selected part of the month.

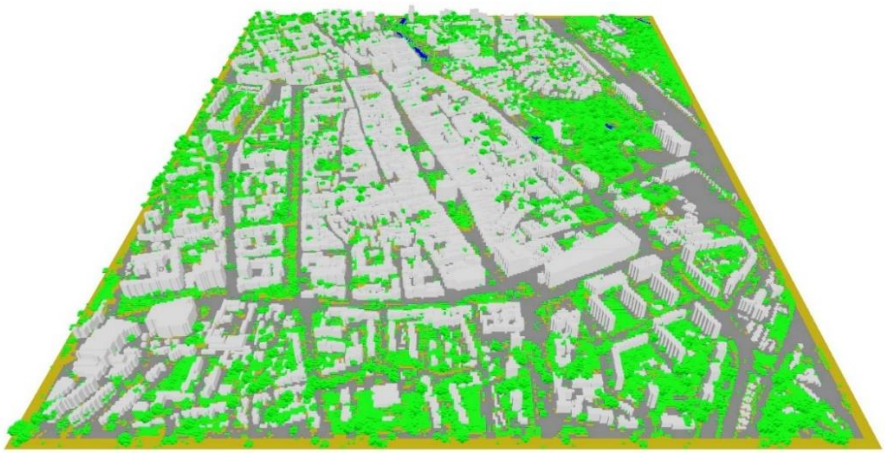

Fig. 2. *3D view of model domain with buildings (grey), tall vegetation (green) and surface type (asphalt – dark grey, brown – bare soil, blue – water)*

The setting of the main dynamic time-step of the computation was set to 2 seconds for sun height below 50° and 1 second for sun height above 50°. The timing update of the processes was 600 seconds for plants, radiation fields, and emissions, 30 seconds for surface processes, and 900 seconds for flow fields. The start of the model run was set to the day before, on 29 June 2022, 12:00 CET to 1 July 2022, 0:00 CET, to ensure proper model spin-up and heat accumulation inside the urban area. Unfortunately, the validation data for this selected date are unavailable because of the lack of stable, high-quality weather measurements inside the city core during this period. However, since the ENVI-met constitutes a widely used model, there are multiple studies demonstrating the model performance with the same or very similar settings and parameterisation (Tsoka et al. 2018, Ayyad and Sharples 2019, Alsaad et al. 2022, Eingrüber et al. 2023).

Input data

For an analysis of a real case study scenario, detailed inputs of the urban morphology are required. The inputs are categorised into several parameterised types implemented in ENVI-met software, consisting of surface type, low vegetation, 3D vegetation, and buildings saved in shapefile format (fig. 3).

Land cover, including categories of low vegetation was categorised using the semi-automatic classification of multispectral Sentinel 2 data and supplied with available shapefiles of road network, water bodies and rivers. The preparation of the land cover classes was conducted using the QGIS SCP plugin (Semi-Automatic Classification Plugin). The workflow and performance of the method are described in several studies, including Leroux et al. (2018) and Tempa and Aryal (2022). For this case study, a simple land cover classification consisting of 5 ENVI-met native classes was prepared, although more classes can be incorporated for use with the model for better representation of the surface (Cilek and Cilek 2021). In our case study, the land cover classes consisted of asphalt (0200ST), railways (0200BA), bare land (000000), low vegetation (0200XX) and deep water (0200WW). The low vegetation class was consequently extracted as an individual layer representing low vegetation (grass). The railway station is in the eastern part of the domain (fig. 3 purple), where also numerous parking lots and large crossroads are located (grey). The city park with dense, tall vegetation can be seen to the right of the city centre, close to the railway station.

The 3D vegetation is represented in the model as a point feature with parameters containing the maximum vegetation height and code of the vegetation describing the trunk width, crown shape, leaf density and type. The 3D vegetation was estimated from LiDAR (Light Detection and Ranging) point cloud data using the lidR package (Roussel et al. 2020) which allows to extract the tree top height as point feature. This method allows for the automation of 3D vegetation preparation over a large area, although it has limitations in classification accuracy and lacks tree type identification. To increase accuracy, the output data were subsequently filtered to remove false 3D vegetation (e.g., building corners, lamps, power lines) by eliminating points associated with built-up infrastructure. The tree type was generalised into six categories of heart-shaped broad-leaf tree regarding its height and trunk size. The height of the trees was generalised into three categories as small (5 m), medium (15 m) and large (25m). The heart-shaped broadleaf tree type was chosen as the predominant tree type in the study area.

The building input is generally prepared in LoD1 (Level of Detail 1), considering the cubic grid of the ENVI-met. Preparation of this data consisted of using the available polygon shapefiles of building footprints with estimated height of the building in attributes. The height was

obtained from a canopy height model derived from the LiDAR point cloud. A median value of the building height was preferred, representing best the prevailing shape and dimensions of the apartment buildings' flat roofs located within the city.

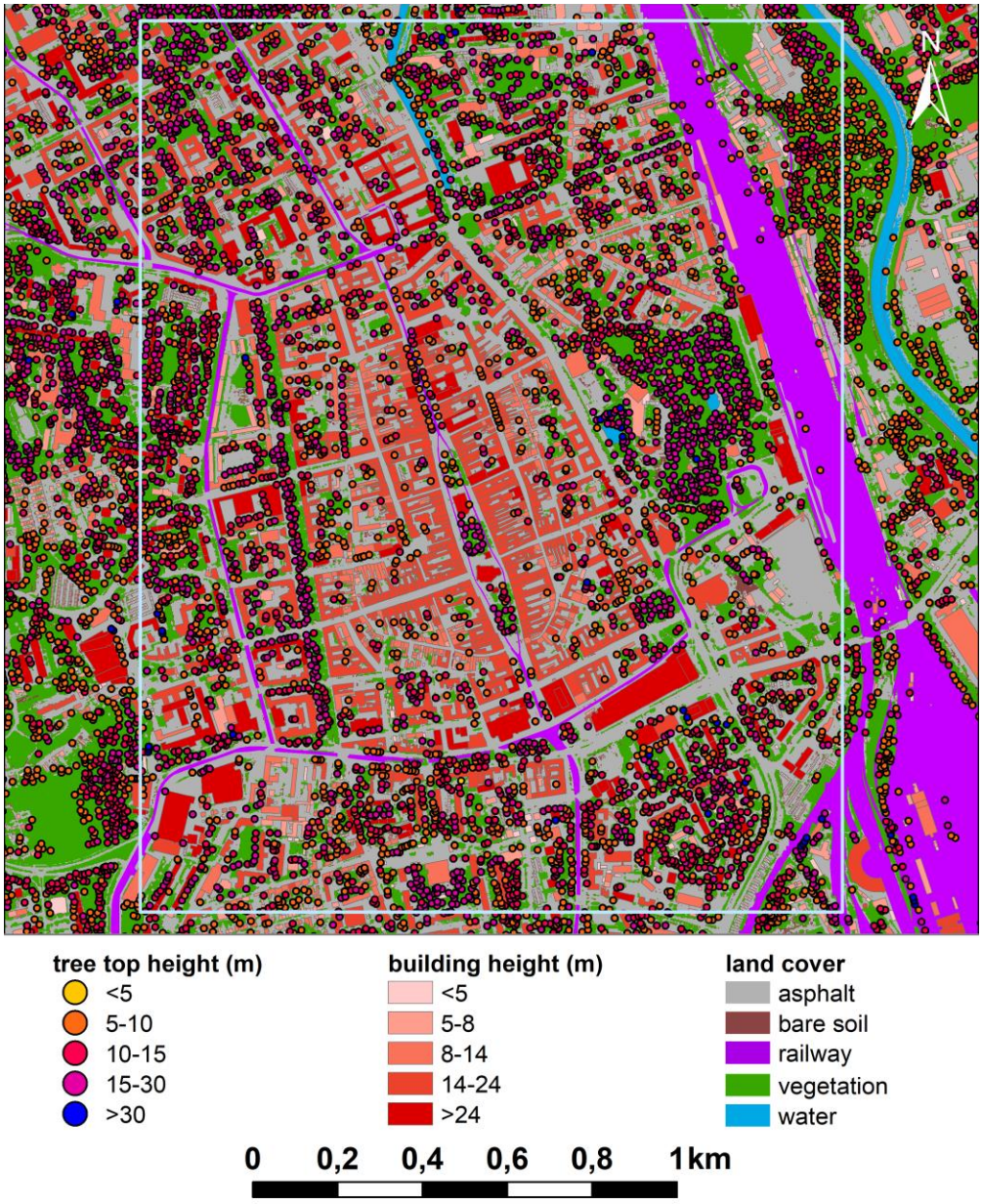

Fig. 3. *Input surface data and model domain (white rectangle) of the Košice city centre*

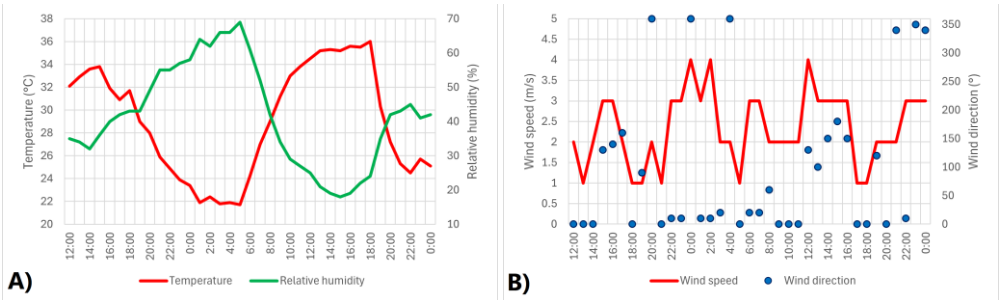

Fig. 4. *Input forcing data of A) 2 m temperature and humidity, and B) 10 m wind speed and direction from SYNOP at the Košice airport between 29 June 2022, 12:00 CET, and 1 July 2022, 0:00 CET*

Thermal comfort assessment

Estimating heat stress is essential for a comprehensive analysis of thermal comfort in urban areas, as it is influenced by multiple atmospheric and environmental variables. Several methods are available for assessing thermal comfort, ranging from those focused solely on atmospheric conditions (Velesa et al. 2019, Awasthi et al. 2022, Brimicombe et al. 2023) to more advanced approaches incorporating human physiological parameters, known as thermo-physiological indices (Höppe 1999, Bröde et al. 2012, Laouadi 2022).

All of the aforementioned thermal comfort estimation methods are highly sensitive to variations in atmospheric variables (temperature, humidity, wind speed, radiation) and may vary significantly depending on weather conditions and the specific location within the city. The physiological parameters can be customised depending on the characteristics of the studied population. Such physiological parameters may include variables like skin temperature, type of clothes, speed of movement, or physical load of the individual.

We selected UTCI (Bröde et al. 2012) as one of the most universal and preferred thermal comfort index for our heat stress assessment in the model domain. The index is widely used in biometeorology, public health, urban planning and safety of the residents to quantify thermal stress across various climates and environments. The main advantage of this index is its universal applicability across all climate types, including cold, hot, humid, dry, and transitional conditions. The UTCI is thermo-physiological index which combine both, environmental and physiological variables as an input. The meteorological variables represent an input of air temperature, mean radiant temperature, wind speed and humidity while the physiological variables are defined as a scale of thermoregulatory response (sweating/shivering), heat exchange, clothing insulation and moisture permeability, core and skin temperature regulation and metabolic rate.

In this study, the UTCI was calculated using Biomet, a subsystem of the ENVI-met model capable of estimating thermal comfort indicators from microscale model outputs with default setting of the physiological parameters. The calculation was run for the height of 1.5 meters representing the height on the pedestrian level. For the estimation of the maximum possible heat stress the late afternoon hours were selected. The late afternoon hours typically reach conditions with highest heat stress because of high heat accumulation, strong short-wave radiation and low wind speeds caused by slowing vertical turbulent mixing within the boundary layer. As such, the 15:00 CET showed the most promising conditions for the heat stress estimation (fig. 5 and fig. 6).

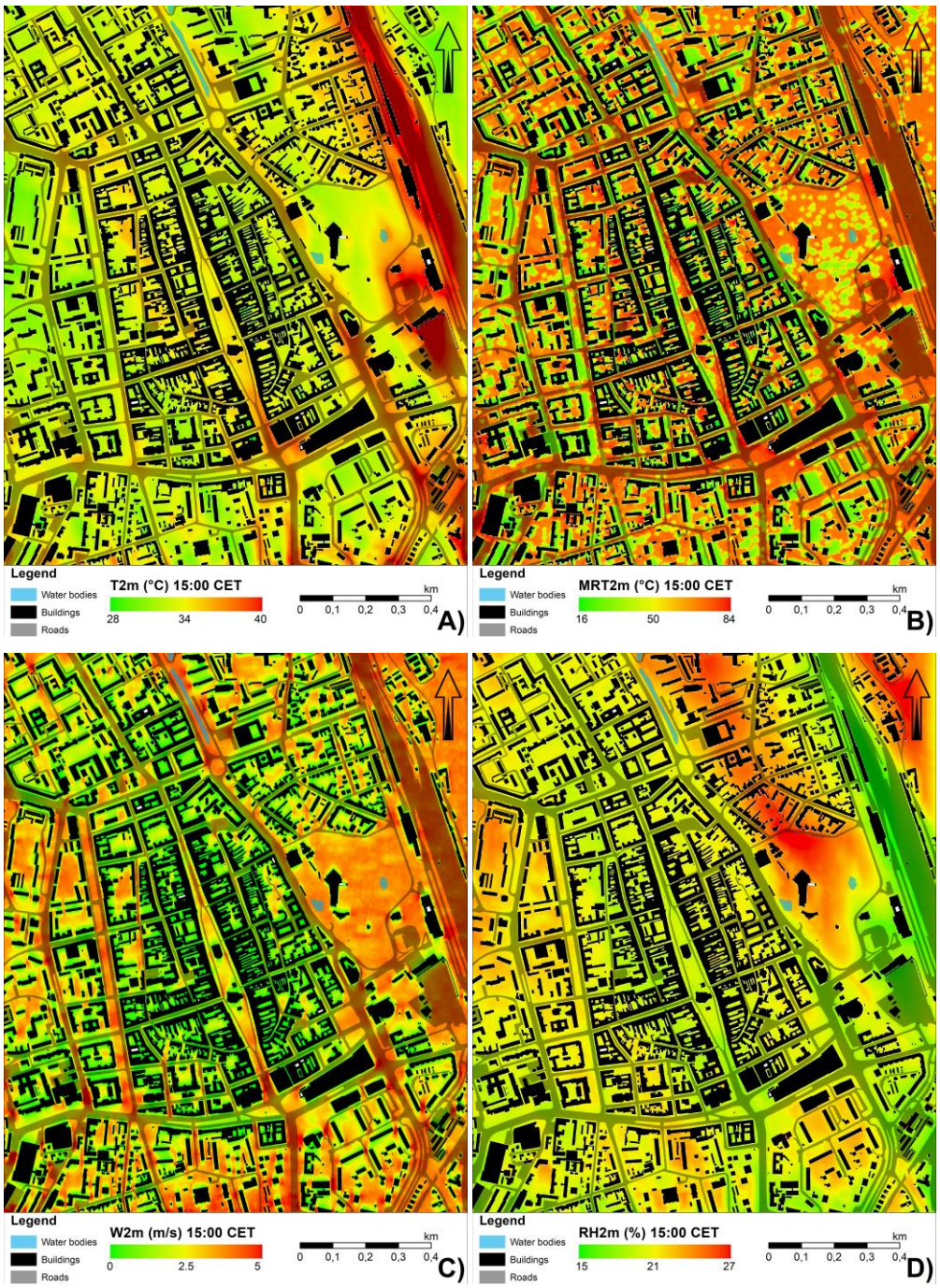

Fig. 5. *A) air temperature (T), B) mean radiant temperature (MRT), C) wind speed (W), D) relative humidity (RH) at 15:00 CET at a pedestrian level (1.5 m) used as input for UTCI*

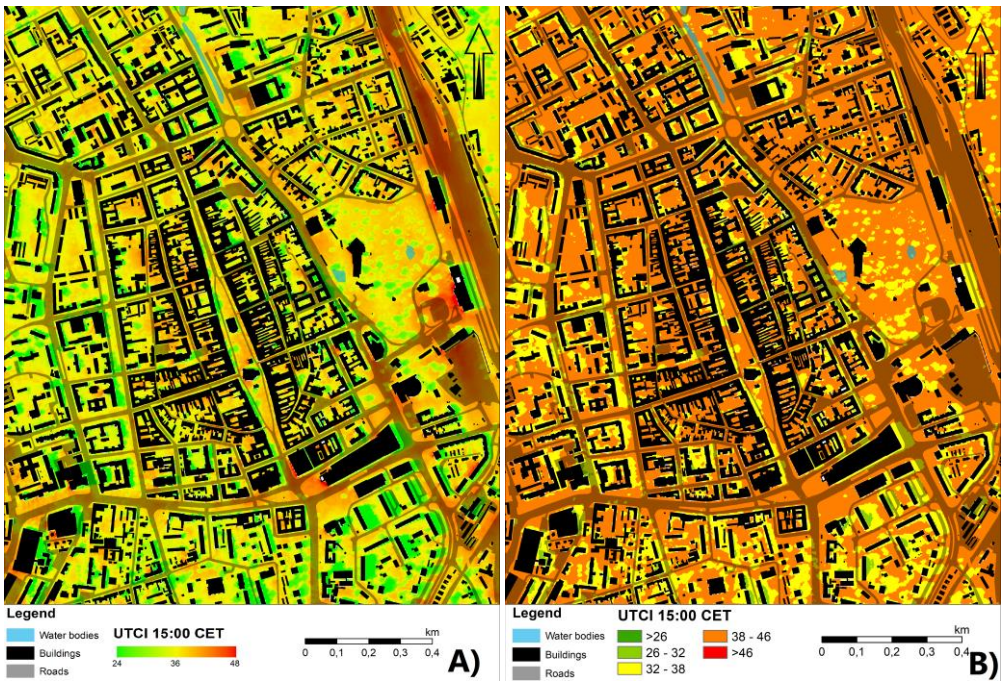

Fig. 6. *A) UTCI at 15:00 CET at a pedestrian level (1.5 m) and B) categorized using the UTCI thresholds values*

Model output interpretation

The calculated UTCI from the high-resolution ENVI-met model run in fig. 6 A) shows a very detailed spatial distribution of the thermal stress in relation to the urban topography. The influence of individual objects is evident, including the shading effects of trees and buildings, as well as the impact of diffuse radiation from taller structures, which increases heat stress on facades oriented toward the sun (south-west orientation). The dense, built-up city centre exhibits moderately high UTCI values for the same reasons and is also characterised by low wind speeds and reduced humidity. Large, open areas covered by built-up surfaces are clearly identifiable as zones of intense overheating. This pronounced overheating is evident over the railway station, nearby parking lots, and large intersections.

The influence of park greenery is also observable, although variations in UTCI are not as pronounced as expected. In the central part of the park, heat stress values are slightly lower only in areas with dense vegetation, but overall remain fairly consistent with those of the surrounding urban environment. The cause of this heat stress distribution can be seen in fig. 5D, where strong evapotranspiration occurs over the city park, creating a humidity plume that advects northward over built-up areas with sparse vegetation. This results in the humid air gradually warming, leading to similar or slightly higher heat stress values compared to the surrounding built-up areas, despite the overall lower air temperature (fig. 5A).

The categorized values of the UTCI (fig. 6 B) are mostly in the range between 38-46, which corresponds to very strong heat stress. Only small areas reach the values of extreme heat stress (>46) and are located close to the facades oriented toward the sun. Strong heat stress (32-38) is observed mostly in the shadows of buildings and trees, with moderate heat stress (23-32) to very locally no heat stress (>26) within the largest building shadows.

Discussion

Microscale models offer a clear advantage over other computational or observational methods focused on the spatial aspects of data when estimating overall thermal comfort in urban areas. With their ability to simulate all relevant environmental and atmospheric variables required for calculating heat stress indices at high resolution, these models present a highly suitable option for localized microclimate simulations. Other approaches, such as NWP models, may achieve greater accuracy in representing atmospheric processes, but are often limited by spatial resolution and computational time (Zhu and Ooka 2023).

ENVI-met and CFD models generally simplify atmospheric processes, focusing primarily on those occurring within the canopy layer. This reduction in complexity significantly decreases the computational demand required for high-resolution simulations. Although these models rely on simplified forcing data and atmospheric conditions, this limitation is generally not problematic when simulating typical UHI scenarios under clear-sky, stable conditions. However, in cases involving specific atmospheric phenomena occurring higher in the atmosphere (e.g., precipitation or convection), or at mesoscale and synoptic scales, NWP models remain more appropriate (Freitag et al. 2018, Nadimpalli et al. 2022).

Another advantage of ENVI-met lies in its capacity to incorporate a highly diverse range of surface morphologies as input for model domains. In our study, we implemented a relatively simplified surface morphology for the city centre, consisting of a few surface types and generalised representations of buildings and 3D vegetation. Nonetheless, additional options – such as the use of customised materials (Faragallah and Ragheb 2022), various surface or vegetation types, and localized sources of heat or water (e.g., fountains) – can be prepared to enhance model detail and improve simulation accuracy.

The ability to modify material types and their parameterisation provides a valuable foundation for designing UHI mitigation strategies (Crank et al. 2018, Cortes et al. 2022). These input data can also be generated using standard geospatial software (GIS), with defined object coordinates and attributes corresponding to ENVI-met classes. Various other methods exist to prepare such high-resolution data over large areas, with customizable parameters and class definitions (Yan et al. 2015, Torresan et al. 2016, Park and Guldmann 2019). This opens new possibilities for high-resolution microclimate simulations at city-wide scales, where manual data preparation would be impractical.

When combined with adequate computational resources, CFD models can perform simulations at horizontal resolutions ranging from several meters to tens of meters across entire urban areas. Such simulations can capture UHI dynamics within the boundary layer and at the interface between urban and surrounding rural areas, thus offering a foundation for future studies that seek to bridge the gap between microscale and mesoscale models – especially where running NWP models in large eddy simulation (LES) mode would be computationally prohibitive. Future research should also aim to quantify the effectiveness of heat-stress mitigation strategies involving modified materials or urban morphology, as these may play a key role in reducing heat stress in urban environments.

Conclusions

In this study, we demonstrated that the use of a CFD-based microscale model can provide a fast and detailed solution for estimating thermal comfort in urban areas. The real-case scenario, conducted at a high spatial resolution of 5 meters, enabled a detailed representation of urban morphology, capturing the shading and evaporative effects of individual objects (e.g., trees, buildings) and identifying hotspots with the highest UTCI values observed during the day over large built-up areas such as the railway station and parking lots.

Dense, built-up areas in the city centre remain among the most vulnerable parts of the urban environment. These zones are characterized by strong heat retention, low wind speeds,

and elevated mean radiant temperatures, caused by a combination of incoming shortwave and emitted longwave radiation from surrounding buildings, often coinciding with high levels of human activity. Due to their dense and frequently historical architecture, the implementation of most mitigation strategies in these areas is typically constrained.

Increased evaporation was observed in the city park, where dense 3D vegetation, fountains, and small ponds contribute to the formation of a humidity-enriched, evaporatively cooled air plume advecting northward (fig. 5A, D). However, as this cooler, humid air moves over adjacent built-up areas, it gradually warms while retaining its high moisture content. This process results in higher UTCI values – up to 2 °C more – compared to the surrounding urban fabric, thereby raising questions about the effectiveness of evaporation-based mitigation strategies under certain conditions.

References

AGHAMOHAMMADI, N., SANTAMOURIS, M. 2022: *Urban overheating: Heat mitigation and the impact on health*. Singapore (Springer). DOI: https://doi.org/10.1007/978-981-19-4707-0.

ALSAAD, H., HARTMANN, M., HILBEL, R., VOELKER, C. 2022: ENVI-met validation data accompanied with simulation data of the impact of facade greening on the urban microclimate. *Data in Brief*, 42, 108200. DOI: https://doi.org/10.1016/j.dib.2022.108200.

AYYAD, Y. N., SHARPLES, S. 2019: Envi-MET validation and sensitivity analysis using field measurements in a hot arid climate. *IOP Conference Series: Earth and Environmental Science*, 329, 012040. DOI: https://doi.org/10.1088/1755-1315/329/1/012040.

AWASTHI, A., VISHWAKARMA, K., PATTNYAK, K. CH. 2022: Retrospection of heat-wave and heat index. *Theoretical and Applied Climatology*, 147, 589-604. DOI: https://doi.org/10.1007/s00704-021-03854-z.

BRANEA, A.-M., DANCIU, M.-I., GAMAN, M. S., BADESCU, S. 2016: Challenges regarding the study of urban heat islands. Ruleset for researchers. In *Risk Reduction for Resilient Cities*, Bucharest.

BRIMICOMBE, CH., LO, CH. H. B., PAPPENBERGER, F., NAPOLI, C. D., MACIEL, P., QUINTINO, T., CORNFORTH, R., CLOKE, H. L. 2023: Wet bulb globe temperature: Indicating extreme heat risk on a global grid. *GeoHealth*, 7(2), e2022GH000701. DOI: https://doi.org/10.1029/2022GH000701.

BRÖDE, P., FIALA, D., BŁAŻEJCZYK, K., HOLMÉR, I., JENDRITZKY, G., KAMPMANN, B., TINZ, B., HAVENITH, G. 2012: Deriving the operational procedure for the universal thermal climate index (UTCI). *International Journal of Biometeorology*, 56, 481-494. DOI: https://doi.org/10.1007/s00484-011-0454-1.

CILEK, M. U., CILEK, A. 2021: Analyses of land surface temperature (LST) variability among local climate zones (LCZs) comparing Landsat-8 and ENVI-met model data. *Sustainable Cities and Society*, 69, 102877. DOI: https://doi.org/10.1016/j.scs.2021.102877.

CORTES, A., REJUSO, A. J., SANTOS, J. A., BLANCO, A. 2022: Evaluating mitigation strategies for urban heat island in Mandaue City using ENVI-met. *Journal of Urban Management*, 11(1), 97-106. DOI: https://doi.org/10.1016/j.jum.2022.01.002.

CRANK, P. J., SAILOR, D. J., BAN-WEIS, G., TALEGHANI, M. 2018: Evaluating the ENVI-met microscale model for suitability in analysis of targeted urban heat mitigation strategies. *Urban Climate*, 26, 188-197. DOI: https://doi.org/10.1016/j.uclim.2018.09.002.

EINGRÜBER, N., KORRES, W., LÖHNERT, U., SCHNEIDER, K. 2023: Investigation of the ENVI-met model sensitivity to different wind direction forcing data in a heterogeneous urban environment. *Advances in Science and Research*, 20, 65-71. DOI: https://doi.org/10.5194/asr-20-65-2023.

FARAGALLAH, R. N., RAGHEB, R. A. 2022: Evaluation of thermal comfort and urban heat island through cool paving materials using ENVI-Met. *Ain Shams Engineering Journal*, 13(3), 101609. DOI: https://doi.org/10.1016/j.asej.2021.10.004.

FEDOR, T., HOFIERKA, J. 2022: Comparison of urban heat island diurnal cycles under various atmospheric conditions using WRF-UCM. *Atmosphere*, 13(12), 2057. DOI: https://doi.org/10.3390/atmos13122057.

FOSTER, J., HODDER, S. G., LLOYD, A. B., HAVENITH, G. 2020: Individual responses to heat stress: Implications for hyperthermia and physical work capacity. *Frontiers in Physiology*, 11, 541438. DOI: https://doi.org/10.3389/fphys.2020.541483.

FREITAG, B. M., NAIR, U. S., NIYOGI, D. 2018: Urban modification of convection and rainfall in complex terrain. *Geophysical Research Letters*, 45(5), 2507-2515. DOI: https://doi.org/10.1002/2017GL076834.

HOFIERKA, J., BOĽARSKÝ, J., KOLEČANSKÝ, Š., ENDEROVÁ, A. 2020a: Modeling diurnal changes in land surface temperature in urban areas under cloudy conditions. *ISPRS International Journal of Geo-Information*, 9, 534. DOI: https://doi.org/10.3390/ijgi9090534.

HOFIERKA, J., GALLAY, M., ONAČILLOVÁ, K., HOFIERKA, J. JR. 2020b: Physically-based land surface temperature modeling in urban areas using a 3-D city model and multispectral satellite data. *Urban Climate*, 31, 100566. DOI: https://doi.org/10.1016/j.uclim.2019.100566.

HÖPPE, P. 1999: The physiological equivalent temperature - a universal index for the biometeorological assessment of the thermal environment. *International Journal of Biometeorology*, 43(2), 5-71. DOI: https://doi.org/10.1007/s004840050118.

HUTTNER, S., BRUSE, M., DOSTAL, P. 2008: Using ENVI-met to simulate the impact of global warming on the microclimate in central European cities. In Mayer, H. and Matzarakis, A. eds. *5th Japanese-German Meeting on Urban Climatology, October 2008*, pp. 307-312. Freiburig (Meteorologischen Instituts der Albert-Ludwigs-Universität). Retrieved from: https://envi-met.net/documents/papers/Huttner_etal_2008.pdf.

CHEVAL, S., DUMITRESCU, A., BIRSAN, M.-V., MARIN, L., POPA, A., POPA, B., BREZA, T. 2021: A systematic review of urban heat island and heat waves research (1991–2022). *Climate Risk Management*, 44, 100603. DOI: https://doi.org/10.1016/j.crm.2024.100603.

KÁNTOR, N., GÁL, C. V., GULYÁS, Á., UNGER, J. 2018: The Impact of Façade Orientation and Woody Vegetation on Summertime Heat Stress Patterns in a Central European Square: Comparison of Radiation Measurements and Simulations. *Advances in Meteorology*, 650642. DOI: https://doi.org/10.1155/2018/2650642.

KOZAK, M., KRUPA, K., HOLOWNIA, M. 2023: Thermal stress comfort in a contemporary housing district in a moderate climate zone, Lublin as a case study. *Budownictwo i Architektura* 22(4), 97-111. DOI: http://dx.doi.org/10.35784/bud-arch.5542.

LAPIN, M., FAŠKO, P., MELO, M., ŠŤASTNY, P., TOMLAIN, J. 2002: Klimatické oblasti (map number 27). In *Atlas krajiny Slovenskej republiky*. Bratislava/Banská Bystrica (Ministry of the Environment of the Slovak Republic and Slovak Environmental Agency). Retrieved from: https://app.sazp.sk/atlassr/.

LAPIN, M., ŠŤASTNÝ, P., TURŇA, M., ČEPČEKOVÁ, E. 2016: High temperatures and heat waves in Slovakia. *Meteorologický časopis* 19(1), 3-10. Retrieved from: https://www.shmu.sk/File/ExtraFiles/MET_CASOPIS/2016-1_MC.pdf.

LAOUADI, A. 2022: A new general formulation for the PMV thermal comfort index. *Buildings*, 12(10), 1572. DOI: https://doi.org/10.3390/buildings12101572.

LEROUX, L., CONGEDO, L., BELLÓN, B., GAETANO, R., BÉGUÉ, A. 2018: Land Cover Mapping Using Sentinel-2 Images and the Semi-Automatic Classification Plugin: A Northern Burkina Faso Case Study. *QGIS and Applications in Agriculture and Forest*, 2. DOI: https://doi.org/10.1002/9781119457107.ch4.

LUO, M., LAU, N.-CH. 2021: Increasing human-perceived heat stress risks exacerbated by urbanization in China: A comparative study based on multiple metrics. *Earth's Future*, 9(7), e2020EF001848. DOI: https://doi.org/10.1029/2020EF001848.

MAHDAVINEJAD, M., SHAERI, J., NEZAMI, A., GOHARIAN, A. 2024: Comparing universal thermal climate index (UTCI) with selected thermal indices to evaluate outdoor thermal comfort in traditional courtyards with BWh climate. *Urban Climate*, 54, 101839. DOI: https://doi.org/10.1016/j.uclim.2024.101839.

MARAS, I., BUTTSTÄDT, M., HAHMANN, J., HOFMEISTER, H., SCHNEIDER, CH. 2014: Investigating public places and impacts of heat stress in the city of Aachen, Germany. *DIE ERDE Journal of the Geographical Society of Berlin*, 144(3-4), 290-303. DOI: https://doi.org/10.12854/erde-144-20.

MEADE, R. D., AKERMAN, A. P., NOTLEY, S. R., MCGINN, R., POIRIER, P., GOSSELINE, P., KENNY, G. P. 2020: Physiological factors characterizing heat-vulnerable older adults: A narrative review. *Environment International*, 144, 105909. DOI: https://doi.org/10.1016/j.envint.2020.105909.

NADIMPALLI, R., PATEL, P., MOHANTY, U. C., ATTRI, S. D., NIYOGI, D. 2022: Impact of urban parameterization and integration of WUDAPT on the severe convection. *Computational Urban Science*, 2, 41. DOI: https://doi.org/10.1007/s43762-022-00071-w.

OKE, T. R. 1982: The energetic basis of the urban heat island. *Quarterly Journal of the Royal Meteorological Society*, 108(455), 1-24. DOI: https://doi.org/10.1002/qj.49710845502.

OLESON, K. W., MONAGHAN, A., WILHELMI, O., BARLAGE, M., BRUNSELL, N., FEDDEMA, J., HU, L., STEINHOFF, D. F. 2013: Interactions between urbanization, heat stress, and climate change. *Climatic Change*, 129, 525-541. DOI: https://doi.org/10.1007/s10584-013-0936-8.

ONAČILLOVÁ, K., GALLAY, M., PALUBA, D., PÉLIOVÁ, A., TOKARČÍK, O., LAUBERTOVÁ, D. 2022: Combining Landsat 8 and Sentinel 2 data in Google Earth Engine to derive higher resolution land surface temperature maps in urban environment. *Remote Sensing*, 14(16), 4076. DOI: https://doi.org/10.3390/rs14164076.

PARK, Y., GULDMANN, J.-M. 2019: Creating 3D city models with building footprints and LIDAR point cloud classification: A machine learning approach. *Computers, Environment and Urban Systems*, 75, 76–89. DOI: https://doi.org/10.1016/j.compenvurbsys.2019.01.004.

ROUSSEL, J. R., AUTY, D., COOPS, N. C., TOMPALSKI, P., GOODBODY, T. R., MEADOR, A. S., BOURDON, J.-F., DE BOISSIEU, F., ACHIM, A. 2020: lidR: An R package for analysis of airborne laser scanning (ALS) data. *Remote Sensing of Environment*, 251, 112061. DOI: https://doi.org/10.1016/j.rse.2020.112061.

SOBOLEWSKI, A., MŁYNARCZYK, M., KONARSKA, M., BUGAJSKA, J. 2020: The influence of air humidity on human heat stress in a hot environment. *International Journal of Occupational Safety and Ergonomics*, 27(1), 226-236. DOI: https://doi.org/10.1080/10803548.2019.1699728.

TEMPA, K., ARYAL, K. J. 2022: Semi-automatic classification for rapid delineation of the geohazard-prone areas using Sentinel-2 satellite imagery. *SN Applied Sciences* 4, 141. DOI: https://doi.org/10.1007/s42452-022-05028-6.

TORRESAN, CH., CORONA, P., SCRINZI, G., MARSAL, J. V. 2016: Using classification trees to predict forest structure types from LiDAR data. *Annals of Forest Research*, 59(2). DOI: https://doi.org/10.15287/afr.2016.423.

TSOKA, S., TSIKALOUDAKI, A., THEODOSIOU, T. 2018: Analyzing the ENVI-met microclimate model's performance and assessing cool materials and urban vegetation applications – A review. *Sustainable Cities and Society*, 43, 55-76. DOI: https://doi.org/10.1016/j.scs.2018.08.009.

VELESA, L., BOJARIU, R., UDRISTIOIU, M. T., SĂRARU, S. C., GOTHARD, M., DASCALU, S. I. 2019: Assessment of summer thermal comfort using the net effective temperature index over Romania. *AIP Conference Proceedings*, 2071(1), 040004. DOI: https://doi.org/10.1063/1.5090071.

XIAO, Y., GAO, Y., WANG, Y., MENG, X. 2020: Effects of solar radiation on thermal sensation and physical fatigue of the human body under heavy-load exercise. *Indoor and Built Environment*, 31(1), 7-16. DOI: https://doi.org/10.1177/1420326X20974736.

YAN, W. Y., SHAKER, A., EL-ASHAMAY, N. 2015: Urban land cover classification using airborne LiDAR data: A review. *Remote Sensing of Environment*, 158, 295-310. DOI: https://doi.org/10.1016/j.rse.2014.11.001.

ZHU, D., OOKA, R. 2023: WRF-based scenario experiment research on urban heat island: A review. *Urban Climate*, 49, 101512. DOI: https://doi.org/10.1016/j.uclim.2023.101512.

Acknowledgement: This research was funded by the Slovak Research and Development Agency (APVV) under the contracts No. APVV-23-0210 and by the Scientific Grant Agency of the Ministry of Education, Science, Research and Sport of the Slovak Republic and the Slovak Academy of Sciences (VEGA) under the contract No. 1/0085/23.

Authors´ affiliations

Tomáš Fedor
Institute of Geography
Faculty of Science, Pavol Jozef Šafárik University in Košice
Jesenná 5, 040 01 Košice
Slovakia
tomas.fedor@student.upjs.sk

Jaroslav Hofierka
Institute of Geography
Faculty of Science, Pavol Jozef Šafárik University in Košice
Jesenná 5, 040 01 Košice
Slovakia
jaroslav.hofierka@upjs.sk